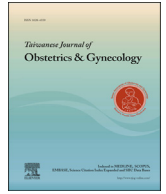




Contents lists available at ScienceDirect

# Taiwanese Journal of Obstetrics & Gynecology

journal homepage: [www.tjog-online.com](http://www.tjog-online.com)

## Original Article

# Frequent and increased expression of human METCAM/MUC18 in cancer tissues and metastatic lesions is associated with the clinical progression of human ovarian carcinoma

Guang-Jer Wu<sup>a, b, \*</sup>, Erin B. Dickerson<sup>c, 1</sup>

<sup>a</sup> Department of Microbiology & Immunology and The Winship Cancer Institute, Emory University School of Medicine, Rollins Research Center, Atlanta, GA 30322, USA

<sup>b</sup> Department of Bioscience Technology, Chung Yuan Christian University, Chung Li 32023, Taiwan

<sup>c</sup> School of Biology and the Ovarian Cancer Institute, Georgia Institute of Technology, Atlanta, GA 30332, USA

## ARTICLE INFO

### Article history:

Accepted 4 March 2014

## ABSTRACT

**Objectives:** Human METCAM/MUC18 (huMETCAM/MUC18), a cell adhesion molecule, plays an important role in the progression of several epithelial cancers; however, its role in the progression of epithelial ovarian cancers is unknown. To initiate the study we determined expression of this protein in normal and cancerous ovarian tissues, cystadenomas, metastatic lesions, and ovarian cancer cell lines.

**Materials and methods:** Immunoblotting and immunohistochemical (IHC) methods were used to determine huMETCAM/MUC18 expression in lysates of frozen and formalin-fixed, paraffin-embedded tissue sections of normal human ovaries, and ovarian (benign) cystadenomas, carcinomas and metastatic lesions. We also determined expression levels of several downstream effectors of METCAM/MUC18 in these tissues.

**Results:** HuMETCAM/MUC18 levels in ovarian carcinomas and metastatic lesions were significantly higher than in normal tissues and cystadenomas. IHC results showed that expression of huMETCAM/MUC18 in normal tissues and cystadenomas was mostly absent from epithelial cells, but in carcinomas and metastatic lesions it was localized to epithelial cells. In higher pathological grades of ovarian cancer and metastatic lesions, the percentage of cells stained in IHC was increased. Thirty percent of normal tissues weakly expressed the huMETCAM/MUC18 antigen, but 70% of cancer tissues and 100% of metastatic lesions expressed the antigen. Expression levels of several downstream effectors of huMETCAM/MUC18, Bcl2, PCNA and VEGF, were elevated in cancerous tissues, however, not that of Bax. The phospho-AKT/AKT ratio was elevated in metastatic lesions.

**Conclusion:** Upexpression of huMETCAM/MUC18 may be a marker for the malignant potential of ovarian carcinomas. Progression of ovarian cancer may involve increased signaling in anti-apoptosis, proliferation, survival/proliferation pathway, and angiogenesis.

Copyright © 2014, Taiwan Association of Obstetrics & Gynecology. Published by Elsevier Taiwan LLC. All rights reserved.

## Introduction

Epithelial ovarian cancer is the fifth most common cancer in women in the United States [1], but it is the most common cause of death from gynecological cancers in this country. Because the early stage of the disease is mostly asymptomatic, diagnosis often occurs after the cancer has already disseminated throughout the

peritoneal cavity [2,3]. The disease can be treated successfully in the early stages, but effective therapy for the advanced stages of the disease is lacking. Currently, the only validated marker, CA125/MUC16, is not useful for diagnosis or prognosis (because of its variability and lack of correlation with the metastatic potential of ovarian cancer) in spite of its presence in the serum of more than 80% of women with ovarian carcinoma [2]. Thus, the major problem for an effective early diagnosis is the lack of reliable diagnostic markers during the cancer progression. Accurate diagnosis is further complicated by the fact that epithelial ovarian carcinomas (90% of the ovarian carcinoma cases) are histologically heterogeneous and lack specific markers for the five major histological

\* Corresponding author. Department of Bioscience Technology, Chung Yuan Christian University, 200 Chung Pei Road, Chung Li 32023, Taiwan.

E-mail addresses: [gjwu@cycu.edu.tw](mailto:gjwu@cycu.edu.tw), [guangj.wu@gmail.com](mailto:guangj.wu@gmail.com) (G.-J. Wu).

<sup>1</sup> Current address: Veterinary Clinical Sciences Department, University of Minnesota, 1352 Boyd Avenue, St. Paul, MN, 55108, USA.

subtypes: serous adenocarcinomas (50% of cases), endometrioid carcinomas (20% of cases), mucinous carcinomas (10% of cases), clear cell adenocarcinomas (5–10% of cases), and transitional cell carcinomas/malignant Brenner tumors [3].

Aberrant expression of cell adhesion molecules (CAMs) affects the motility and invasiveness of many tumor cells *in vitro* and metastasis *in vivo*, because CAMs govern the social behaviors of cells by affecting the adhesion status of cells and modulating cell signaling [4]. The metastatic potential of a tumor cell, as documented in many carcinomas, is actually the consequence of a complex participation of many over- and underexpressed CAMs [4]. Likewise, CAMs play a very important role in regulating ovarian cancer migration and attachment to the omentum, pelvic peritoneum, bowel serosa, diaphragm, liver serosa, para-aortic and pelvic lymph nodes, and the establishment of metastatic lesions [5,6]. The effects of altered expression of CAMs on the metastasis of ovarian cancer cells has been studied in relation to mucins [7], integrins [8], CD44 [9], L1CAM [10], E-cadherin [11], and claudin-3 [12]; however, that of human METCAM/MUC18 (huMETCAM/MUC18) has not been investigated.

METCAM/MUC18 is a CAM in the immunoglobulin gene super family [13,14]. The ectodomain of METCAM/MUC18 probably mediates the direct interactions with other cell types and the extracellular matrix [13,14]. The cytoplasmic domain (64 amino acids) of huMETCAM/MUC18 contains consensus sequences for five phosphorylation sites, one PKA, one casein kinase II (CK2), and three protein kinase Cs (PKCs) [13,14]. The protein structure of huMETCAM/MUC18 suggests that it plays an active role in crosstalk with many intracellular signaling pathways, thus impacting cellular behaviors [13,14].

HuMETCAM/MUC18 is normally expressed in several tissues, such as hair follicular cells, smooth muscle cells, endothelial cells, cerebellum, normal mammary epithelial cells, basal cells of the lung, intermediate trophoblast, and some activated T cells [15]. The protein is frequently overexpressed in most (67%) malignant melanoma cells [14] and in most (more than 80%) of the prostate epithelial cells in PINs, high-grade prostatic carcinoma cells, and metastatic lesions [16–19]. Furthermore, the effect of huMETCAM/MUC18 expression on different tumor cells may vary; for example, in melanoma huMETCAM/MUC18 has a minimal effect on tumorigenesis, yet promotes the metastasis of melanoma cells, albeit at the later stages [20–23]. In contrast, huMETCAM/MUC18 increases tumorigenesis and initiates metastasis of human prostate cancer LNCaP cells [24–26] and breast cancer cells [27–29]. Thus huMETCAM/MUC18 is a *bona fide* metastatic gene for these cancers [14]. In addition, more evidence seems to support the notion that huMETCAM/MUC18 also plays an important role in promoting the metastasis of other cancer types, such as angiosarcomas [14] and osteosarcomas [30]. As a result, it is highly possible that huMETCAM/MUC18 may also play an important role in initiating the metastasis of ovarian cancer cells, because it is well documented that cancers from different tissues express some common cancer-promoting genes in addition to tissue-specific genes [31].

To test the above hypothesis, we used immunological methods to determine the expression of huMETCAM/MUC18 in normal human ovaries, cystadenomas, cancerous ovaries, and metastatic lesions. In this report, we show that huMETCAM/MUC18 was overly expressed in ovarian cancer and ovarian metastatic lesions compared to normal ovarian and cystadenoma tissues, suggesting that the overexpression of huMETCAM/MUC18 may be used as a diagnostic marker for differentiating cancerous ovaries from normal ovaries and from benign ovarian cystadenomas. We also determined the expression levels of an apoptosis index (Bax), an anti-apoptosis index (Bcl2), a proliferation index (proliferating cell nuclear antigen [PCNA]), a survival and growth pathway index (phosphor-AKT/

AKT), and an angiogenesis index (vascular endothelial growth factor [VEGF]) in lysates of tumors and metastatic lesions. We show that the levels of Bcl2, PCNA, and VEGF were elevated in lysates of tumors, and the phospho-AKT/AKT ratio was elevated in metastatic lesions, suggesting that these signaling pathways were involved in the malignant progression of ovarian cancer.

## Materials and methods

### Ovarian tissues

Ovarian tissues were obtained from Northside Hospital given to Ovarian Cancer Institute/Georgia Institute of Technology, Atlanta, GA, and 5- $\mu$ m sections of paraffin-embedded ovarian cancer tissues were obtained from Emory University Hospital, Atlanta, GA. All studies using human tissue were approved by institutional review boards at both the Georgia Institute of Technology and Emory University.

### Growth of ovarian cancer cell lines

A SV40-T antigen immortalized human normal ovarian epithelial cell line, IOSE [32] obtained from Dr Nelly Auersperg, Vancouver, Canada, was maintained in M199/MCDB105 (1:1) medium supplemented with 15% fetal bovine serum and 50  $\mu$ g/mL of gentamicin. The human ovarian cancer cell line BG-1 [33] (provided by Dr Nathan Bowen, School of Biology, and the Ovarian Cancer Institute, Georgia Institute of Technology) was maintained in DMEM/F12 medium supplemented with 10% fetal bovine serum. The human ovarian cancer cell line Hey [34] (provided by Dr Gordon Mills, Department of Molecular Therapeutics, MD Anderson Cancer Center) was maintained in a modified RPMI 1640 medium supplemented with 25mM HEPES buffer, 1mM sodium pyruvate, 1mM glutamine, 4.5% glucose, and 10% fetal bovine serum. Human ovarian cancer cell lines, CAOV-3 and NIH:OVCAR-3 (or OVCAR3) from ATCC were maintained in DMEM supplemented with 10% fetal bovine serum and a modified RPMI 1640 medium supplemented with 25mM HEPES buffer, 1mM sodium pyruvate, 1mM glutamine, 4.5% glucose, 20% fetal bovine serum 10  $\mu$ g/mL of bovine insulin, respectively. Human ovarian cell lines SK-OV-3 and CAOV-4 from the American Type Culture Collection (ATCC), which were originally established from ovarian metastatic lesions, were maintained in McCoy's 5A medium supplemented with 10% fetal bovine serum and Leibovitz's L-15 medium supplemented with 20% fetal bovine serum, respectively. All the media were supplemented with penicillin, streptomycin, and amphotericin B except the medium for the IOSE cell line. The media were obtained from Invitrogen/Life Technology/GIBCO/BRL or Cellgro/MediaTech, Carlsbad, CA, USA. Fetal bovine serum was from Cellgro/MediaTech, Manassas, VA, USA. All the cell lines were maintained in a 37°C incubator with 5% CO<sub>2</sub>, except CAOV-4, which was maintained in a 37°C incubator without CO<sub>2</sub>.

### Immunoblot analysis

Lysates of ovarian tissues were prepared similarly to the procedures previously described [16–19,24,25]. The protein concentration of each lysate was determined and verified by gel electrophoresis and staining as described [16–19,24,25]. A 20–30  $\mu$ g sample of protein from each tumor lysate was loaded in each lane. The standard procedure of immunoblot analysis with minor modifications was used [16–19,24,25]. The primary antibody used for immunoblotting of METCAM/MUC18 protein was chicken anti-huMETCAM/MUC18 IgY, which was obtained by immunizing chickens with the purified middle portion of the recombinant

huMETCAM/MUC18 protein expressed in *Escherichia coli* [17–19,23–25]. The anti-huMETCAM/MUC18 polyclonal antibody had a high specificity for recognizing the epitopes of huMETCAM/MUC18 and a minimal cross-reactivity with the epitopes of mouse METCAM/MUC18 [17–19,23–25].

In brief, after electrical blot the nitrocellulose membrane (Hybond ECL, RPN3032D, GE Healthcare/Amersham) was blocked with 5% nonfat milk–Tris-buffered saline with Tween-20 (TBST)–sodium azide at room temperature for 2 hours and reacted with 1/200–1/300 dilution of a primary antibody (chicken anti-huMETCAM/MUC18 IgY) in 5% nonfat milk–TBST–sodium azide at 4°C for 4–6 hours or overnight. The membrane was washed with TBST, and reacted with 1/2000 dilution of a secondary antibody (AP-conjugated rabbit anti chicken IgY antibody, AP162A, Chemicon) at room temperature for 1 hour. The membrane was washed again with TBST, and reacted with NBT/BCIP for about 10–15 minutes, until the purple color of the protein band was fully developed. The image of the huMETCAM/MUC18 band from each specimen was scanned with an Epson Photo Scanner model 1260 and its intensity was quantitatively determined by a NIH Image J program version 1.31.

A dilution of 1/200 of the primary antibodies against human Bcl-2 (N-19) (SC-492, rabbit polyclonal antibody, Santa Cruz Biotech), Bax (N-20) (SC-493, rabbit polyclonal antibody, Santa Cruz Biotech), anti-PCNA (C-20) (SC-9857, goat polyclonal antibody, Santa Cruz Biotech), and anti-human VEGF (147) (SC-507, rabbit polyclonal antibody, Santa Cruz Biotech) was used for the immunoblot analyses of the above proteins. A 1/2500 dilution of anti-pan-AKT (AF2055, rabbit polyclonal antibody, R&D Systems, Inc.) and a 1/2000 dilution of anti-phospho (Ser473)-AKT antibody (AF-887, rabbit polyclonal antibody, R&D Systems, Inc.) were used for the immunoblot analyses of the AKT and phospho-AKT. Dilutions of the corresponding AP-conjugated secondary antibodies, rabbit anti-chicken IgY (AP162A, Chemicon), rabbit anti-goat (AP106 A, Chemicon), rabbit anti-mouse (AP160A, Chemicon), or goat anti-rabbit (AP132A, Chemicon) were all 1/2000. The color development substrate BCIP/NBT (S3771, Promega) was used for the color reaction for 30 minutes or overnight. The image of the specific protein band on the membrane was scanned by the above scanner and its intensity was quantitatively determined as described above. All the data were statistically analyzed using the Student *t* test.

#### *Histology and immunohistochemistry of ovarian tissue sections*

Paraffin-embedded tissue sections (5 μm) were used. Tissue sections were de-paraffinized, rehydrated, and used for histological staining or immunohistochemical analyses [16–19,24,25]. For histology, a standard procedure of staining with acidified Harris hematoxylin (#S212A, Poly Scientific, #245-677, Protocol, or #23-245677, Fisher) and eosin philoxine (#S176, Poly Scientific), or Eosin Y intensified solution (# 314-630, Protocol or #23-314-630, Fisher), was used [25]. For the IHC with anti-huMETCAM/MUC18 antigens, sections of a human melanoma tissue and a tumor derived from an LNCaP-expressing clone (LNS239) [25] were used as positive external controls. Antigen-retrieval was carried out by gentle boiling in a 20mM sodium citrate buffer (pH 6.0) at 95–97°C for 10 minutes and cooled for 60 minutes (temperature dropped from 95°C to about 37–42°C) [16–19,24,25]. The endogenous peroxidase was quenched with 3% hydrogen peroxide for 10 minutes. All tissue sections were blocked with 5% nonfat milk in TBST with 0.02% sodium azide at room temperature for 2 hours and followed at 4°C for overnight, and reacted with the primary antibodies (1/200–1/400 dilutions of the chicken anti-huMETCAM/MUC18 IgY in 5% nonfat milk in TBST with and 0.02% sodium azide) for 50 min at room temperature [25]. A secondary antibody

(1/250 dilution of the biotin-conjugated rabbit anti-chicken IgY antibodies, G2891, Promega, in freshly made 5% nonfat milk in TBST without sodium azide) was incubated for 30 minutes at room temperature, a streptavidin-conjugated horseradish peroxidase complex (K1016, Dako LSAAB-2 system) for 45 minutes, and diaminobenzidine as the chromogen for 20 minutes. The tissue sections were then counterstained with acidified Harris hematoxylin (#245-677 Fisher) for 2 to 3 minutes. All the incubations were performed at room temperature. Between incubations, sections were washed three times with TBST. For negative controls, the primary antibody was replaced by nonfat milk, chicken IgY, or anti-mouse METCAM/MUC18 polyclonal antibodies (1/300 dilution). All the tissues sections were dehydrated sequentially in increasing concentrations of ethanol (50%, 70%, 80%, and 95%), followed by three soakings in 100% ethanol, and three soakings in xylene. Coverslips were mounted on the slides with a mounting medium containing xylene-based synthetic resin (#S2153, Poly Scientific or #245-690, Protocol or #23-245690, Fisher).

#### *Statistical analysis*

The calculation of standard deviations and the Student *t* test (one-tail and type 2) in Microsoft Excel was used to analyze the statistical significance of the data in all figures. Two corresponding sets of data were considered to be significantly different if the *p* value was <0.05.

## **Results**

#### *Expression of huMETCAM/MUC18 in ovarian tissues*

Because huMETCAM/MUC18 promotes tumorigenesis and initiates metastasis of human breast and prostate cancer cells (cancers of an epithelial cell origin) we sought to determine if huMETCAM/MUC18 was also more highly expressed in epithelial ovarian cancer and if the expression was associated with the clinical progression of this disease. Using ONCOMINE, a public cancer microarray and web-based data-mining platform ([www.oncomine.org](http://www.oncomine.org)), we determined that the levels of expression of huMETCAM/MUC18 were higher in neoplastic versus normal ovarian tissues (data not shown). DNA microarray analysis of normal ovarian surface epithelia (NOSE) and epithelial ovarian carcinoma (EOC) samples from one of our laboratories indicated at least a 3-fold increase of huMETCAM/MUC18 in EOC when compared to NOSE (data not shown).

To follow up the results from the DNA microarray data, we used immunoblotting techniques to determine the protein expression levels of huMETCAM/MUC18 in several normal tissue, benign tissue, cancerous tissue, and metastatic lesion specimens. Fig. 1 shows a moderate expression of huMETCAM/MUC18 in normal ovarian tissues, a high expression in all (100%) ovarian cancer tissues, and moderate expression in all (100%) metastatic lesions; however, a very weak expression of the protein in cystadenomas. The huMETCAM/MUC18 levels in normal ovarian tissues, cancerous ovarian tissues, and metastatic lesions were 3.6 ( $p = 0.02$ ), 10.4 ( $p = 0.007$ ), and 4 ( $p = 0.0085$ ) times that in cystadenomas, respectively (Fig. 1B). Thus the expression level of the huMETCAM/MUC18 protein in cancerous ovarian tissues was 2.9-fold higher than that in normal ovarian tissues and 10.4-fold higher than that in cystadenomas. The expression level of the huMETCAM/MUC18 protein in cancerous ovarian tissues was 2.6-fold higher than that in metastatic lesions. Furthermore, the apparent electrophoretic mobility of huMETCAM/MUC18 expressed in ovarian tissues was similar to that in a human melanoma cell line, SK-Mel-28, and human melanoma, prostate, breast cancer, and bladder cancer cell lines.



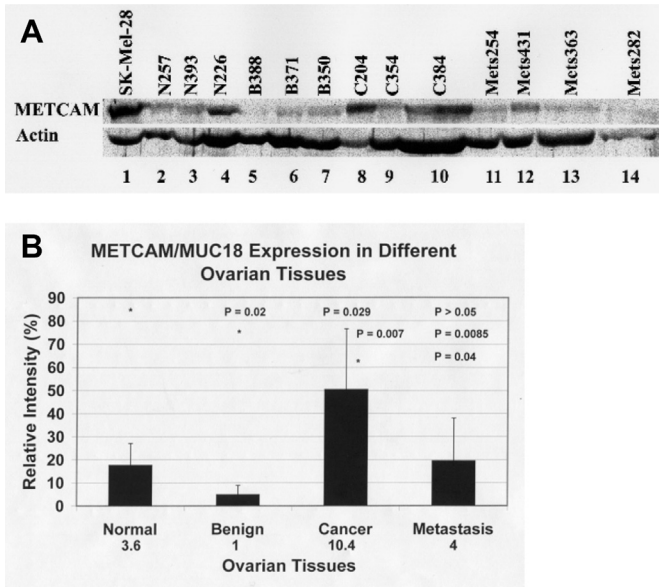


**Fig. 1.** Expression of huMETCAM/MUC18 protein in normal, benign, cancerous, and ovarian metastatic lesions. (A) Results of immunoblot analyses of the ovarian tissues; 20  $\mu$ g protein of each tumor lysate or cell line lysate was loaded per lane. The expression of huMETCAM/MUC18 protein in a human melanoma cell line, SK-Mel-28, was used as a positive control. Actin was used as the loading control. (B) Quantitative results of the immunoblot analyses in (A). The expression level of huMETCAM/MUC18 protein in a human melanoma cell line, SK-Mel-28, was assumed to be 100%. The *p* values were calculated by using the data of benign (cystadenomas), or normal ovarian tissues, or cancerous tissues as the reference.

To confirm the immunoblot results and further locate the expression of huMETCAM/MUC18 in different cell types, IHC of paraffinized tissue sections of normal ovaries, ovarian cystadenomas, ovarian cancers, and ovarian metastatic lesions was carried out, as shown in Fig. 2A and that in different stages of ovarian cancers, as shown in Fig. 3A. The antigen of huMETCAM/MUC18 was expressed mostly in the smooth muscle cells and vasculature in normal ovarian tissue sections and in cystadenomas, as shown in Figs. 2A and 3A. In contrast, the huMETCAM/MUC18 antigen was expressed in a greater majority of cells and at higher levels in most of the cancer tissue sections and metastatic lesions (Figs. 2A and 3A). Note that the apparent levels of huMETCAM/MUC18 analyzed by immunoblot analyses were lower in metastatic lesions than in cancer tissues (Fig. 2A). The quantitative results of IHC are shown in Fig. 2B, indicating that the percentage of cells stained by the anti-huMETCAM/MUC18 antibody was higher in both cancerous tissues ( $p = 0.011$ ) and metastatic lesions ( $p = 0.017$ ) in comparison with normal tissues and cystadenomas. Fig. 3A shows similar observations when tissue sections were from different clinical stages and Fig. 3B shows that the percentage of cells stained by the anti-huMETCAM/MUC18 antibody was at the highest in the pathological Grade III cancers and in the metastatic lesions in comparison with normal tissues and lower pathological grades of ovarian cancer; however not much difference between the pathological Grade III and metastatic lesions ( $p > 0.05$ ). Table 1 summarizes the results of the IHC of the expression of huMETCAM/MUC18 in these tissues, showing that huMETCAM/MUC18 was expressed in about 85% of the ovarian cancer tissues and 100% of ovarian metastatic lesions, but only 30% of normal ovarian tissues.

The METCAM/MUC18 antigens were also expressed in most (83%) serous carcinomas (stage IIIC), one serous carcinoma with a transitional differentiation, one mucinous carcinoma with a known low malignant potential, one ovarian adenocarcinoma (Stage IC), and one mixed type epithelial ovarian cancer (Stage IIIC). The

expression of the METCAM/MUC18 antigen was significantly detectable in a low malignant potential serous ovarian cancer and in adenocarcinoma. In contrast it was not expressed in one mucinous adenocarcinoma and in one serous carcinoma (Stage IIIA), but weakly expressed in 50% of the endometrioid carcinomas (data not shown).

#### Expression of huMETCAM/MUC18 in various ovarian cancer cell lines

The levels of huMETCAM/MUC18 expressed in various ovarian cancer cell lines ranged a great deal, from 5 to 50%, when compared to a positive control, the human melanoma cell line SK-MEL-28 (assuming to be 100%). SK-MEL-28 was used as a positive control because it has the highest expression level of METCAM/MUC18 documented to date. One cell line, BG-1, did not express any huMETCAM/MUC18 (Fig. 4 and Table 2). As summarized in Table 2, the apparent average relative expression level of huMETCAM/MUC18 in the cell lines derived from ovarian carcinomas was 25.6%, about twice of that observed in cell lines derived from the malignant ascites/metastases (13.3%), appearing to be similar to our above observations for ovarian cancer tissues and ovarian metastatic lesions. As also shown in Fig. 4, the apparent electrophoretic mobility of huMETCAM/MUC18 expressed in ovarian cancer cell lines was similar to that in a human melanoma cell line, SK-Mel-28, and human melanoma, prostate, breast cancer, and bladder cancer cell lines. Taken together of all the results, we were certain that huMETCAM/MUC18 was expressed in the cell lines derived from ovarian cancers and metastatic lesions, though the expression level varied greatly in different cell lines.

#### Expression of various signaling parameters downstream of huMETCAM/MUC18 in ovarian tissues

HuMETCAM/MUC18 has been shown to affect many important downstream factors, such as proliferation, survival signaling, angiogenesis, and apoptosis, which control tumorigenesis and metastasis [14,35]. To understand the contribution of these key signaling molecules in the processes of tumorigenesis and metastasis of ovarian carcinomas, the levels of apoptosis indexes, PCNA, phospho-AKT, and VEGF in the lysates made from frozen tissues of normal ovary, benign cystadenomas, ovarian cancers, and metastatic lesions in ovaries were determined by immunoblot analyses using specific antibodies. As shown in Fig. 5A, Bcl-2 levels were higher in cancerous tissues than in the other kinds of tissue. In contrast, the Bax level was similar in all four types of ovarian tissues, as shown in Fig. 5B. The level of PCNA was significantly higher ( $p < 0.01$ ) in cancerous tissues than in all other kinds of tissues; it was significantly higher in metastatic lesions ( $p < 0.01$ ) than in normal ovarian tissues and cystadenomas, as shown in Fig. 6. The level of activated AKT (phospho-AKT) was higher in metastatic lesions than in three other kinds of tissues, as shown in Fig. 7. The level of the active form of VEGF (21kDa) was slightly higher in cancerous tissues than in other three kinds of tissues, as shown in Fig. 8.

Taken together, levels of Bcl-2, PCNA, and VEGF were significantly higher in cancerous tissues and phospho-AKT was significantly higher in metastatic lesions than in normal ovarian tissues and benign cystadenomas.

#### Discussion

In this report, we showed from immunoblot results that the expression level of the huMETCAM/MUC18 protein in cancerous ovarian tissues was significantly higher (2.9-fold) than that in normal ovarian tissues, consistent with our DNA microarray

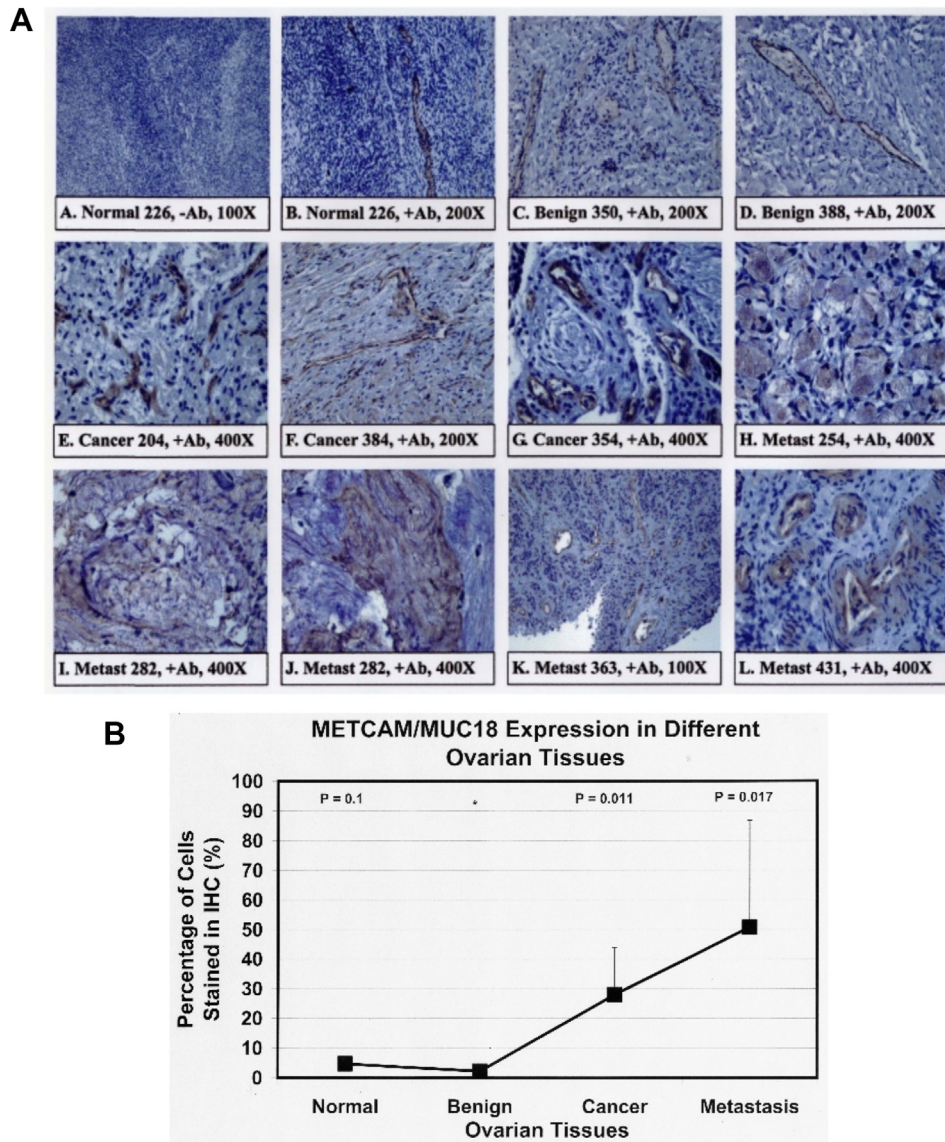


**Fig. 2.** Immunohistochemistry (IHC) of the expression of huMETCAM/MUC18 in normal, cystadenoma, ovarian cancer, and metastatic ovarian tissues. (Panel A) Results of IHC: (A,B) shows representative examples of IHC for normal ovarian tissues, (C,D) cystadenomas, (E–G) ovarian cancers, and (H–L) metastatic lesions. Controls without the primary antibody are shown in (A) and (C). (Panel B) Quantitative results of IHC in panel A. The average percentage of cells positively stained with the anti-huMETCAM/MUC18 antibody in five to 17 microscope fields was plotted against various ovarian tissues. The *p* values were calculated using the data of cystadenoma as the reference.

analysis in which the expression of the huMETCAM/MUC18 mRNA in ovarian cancer tissues is about 3-fold higher than in normal ovarian tissues. This suggests that elevated huMETCAM/MUC18 may be used for the clinical diagnosis of the emergence of ovarian cancers. The expression level of the huMETCAM/MUC18 protein in cancerous ovarian tissues was also significantly higher than in cystadenomas, suggesting that elevated huMETCAM/MUC18 may also be used as a diagnostic biomarker in clinics to differentiate ovarian cancers from benign cystadenomas.

To further confirm the results of immunoblot analyses and to establish the cell types that express huMETCAM/MUC18, we showed in IHC that the expression of huMETCAM/MUC18 in normal ovarian tissues and cystadenomas was mostly located in the smooth muscle cells and vasculature, but not in epithelial cells. In contrast, the expression of huMETCAM/MUC18 in the cancers and metastatic lesions was mostly located in the ovarian epithelial cells. This was further corroborated by the quantitative IHC results that the expression level of huMETCAM/MUC18 antigen in ovarian

tissues was higher in cancerous tissues, metastatic lesions, and the high pathological grade of ovarian cancers than in normal tissues and lower grades of ovarian cancers.

We also noticed that the average huMETCAM/MUC18 level in cell lines derived from primary tumors was about twice of that found in ovarian carcinoma cell lines derived from metastatic lesions or ascites fluid. This appeared to be consistent with the results of immunoblot analysis that the expression level of huMETCAM/MUC18 in ovarian cancerous tissues was 2.6-fold higher than in metastatic lesions. However, this consistency may be somewhat misleading, for several reasons. First, the expression levels between two groups of cell lines was not statistically different; therefore the 2-fold difference of expression levels between the two groups of cell lines was not considered meaningful. Second, immunoblot analysis only detects the total expression level of a particular protein in a tissue lysate and does not differentiate between the expression of a protein from one cell type to another. Because huMETCAM/MUC18 is also expressed in the stromal cells, such as



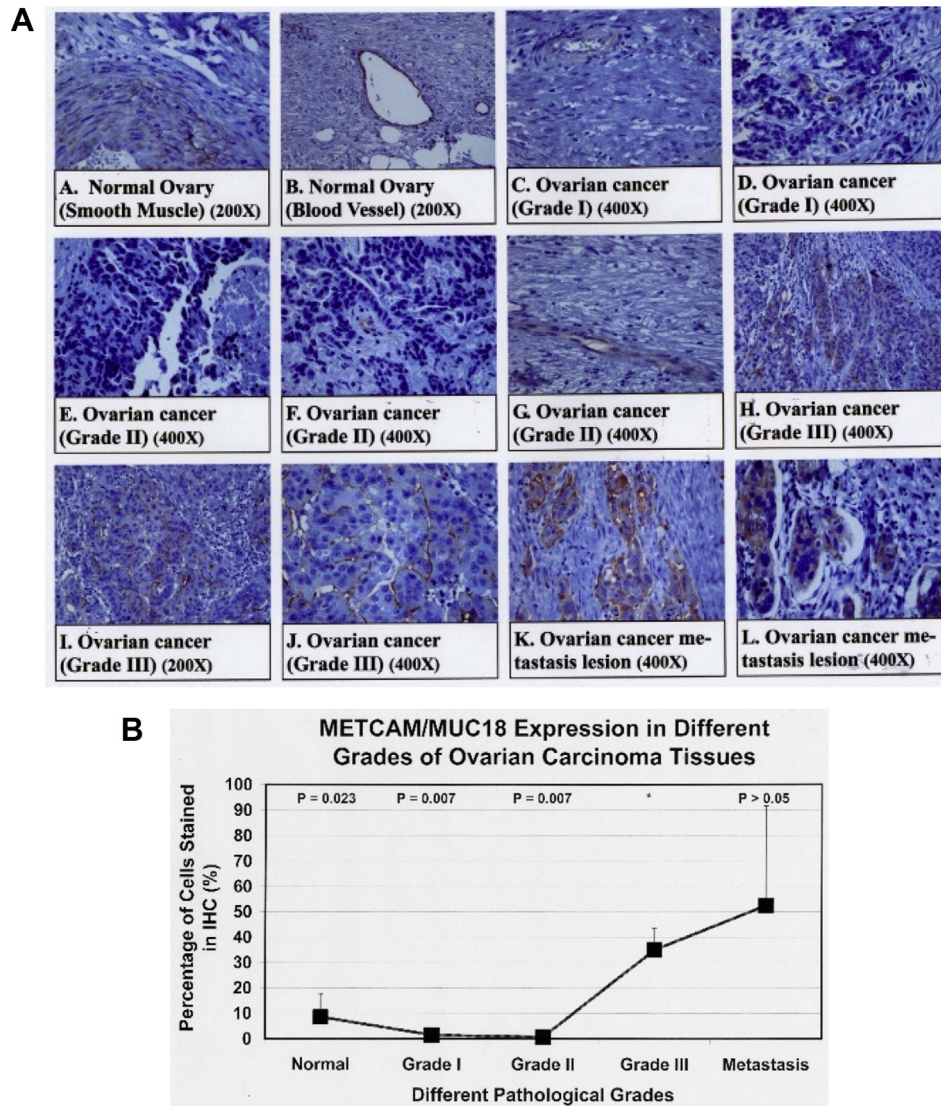


**Fig. 3.** Immunohistochemistry (IHC) of huMETCAM/MUC18 expression in normal, different grades of ovarian cancerous and metastatic ovarian tissues. (Panel A) Results of IHC: (A,B) shows the typical IHC of normal ovarian tissues, (C,D) Grade I ovarian cancers, (E–G) Grade II ovarian cancers, (H–J) Grade III ovarian cancers, and (K,L) metastatic lesions. (Panel B) Quantitative results of IHC in panel A. The average percentage of cells positively stained with the anti-huMETCAM/MUC18 antibody in five to 17 microscope fields was plotted against normal and different grades of ovarian cancer. The *p* values were calculated by comparing the data from all different tissues to the data of Grade III ovarian cancer tissues as the reference.

muscle cells and endothelial cells in the vasculatures, these non-epithelial cells may contribute to the total level of the total lysates of cancerous tissues, whereas they do not contribute to the total level of expression in metastatic lesions. Thus immunoblot analysis

likely over-scored the contribution of METCAM/MUC18 expression from epithelial cells in ovarian cancerous tissues to the total level. This problem is resolved by the IHC analysis, which does differentiate between the expressing METCAM/MUC18 from one cell type

**Table 1**  
HuMETCAM/MUC18 expression in the epithelium of the normal ovary, ovarian cancer, and metastatic lesions.

Histological/pathological classification	Number of cases negative for huMETCAM/MUC18 expression (%)	Number of cases positive for huMETCAM/MUC18 expression (+1) <sup>a</sup> (%)	Number of cases positive for huMETCAM/MUC18 expression (+2) <sup>a</sup> (%)	Number of cases positive for huMETCAM/MUC18 expression (+3) <sup>a</sup> (%)	Number of cases positive for huMETCAM/MUC18 expression (%)
Normal ovary (n = 10)	7 (70)	3 (30)	0	0	3/10 (30)
Cancer (n = 27) <sup>b</sup>	8 (30)	7 (26)	7 (26)	5 (18)	19/27 (70)
Metastasis (n = 6)	0	1 (17)	1 (17)	4 (66)	6/6 (100)

<sup>a</sup> The intensity and percentage of cells positive for the staining of huMETCAM/MUC18 is defined as: +1, 5–10%; +2, 20–30%; and +3, 40–80%.

<sup>b</sup> Twenty-seven ovarian cancer specimens include 17 serous adenocarcinoma, six endometrioid carcinomas, two mucinous carcinomas, and two mixed subtypes of ovarian carcinomas.

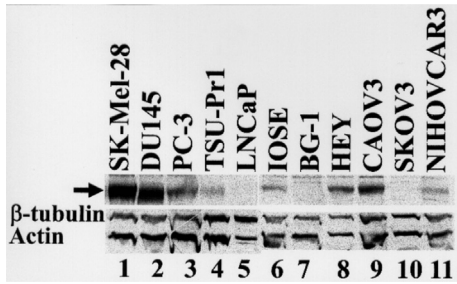


**Fig. 4.** Expression of huMETCAM/MUC18 in ovarian cancer cell lines versus a human melanoma cell line (SK-Mel-28) and human prostate cancer cell lines (DU145, PC-3, and LNCaP) and a human bladder cancer cell line (TSU-Pr1); 20 µg protein of each cell line lysate was loaded per lane for immunoblot analysis. The top row shows the expression of huMETCAM/MUC18 in a human melanoma cell line (SK-Mel-28 in lane 1), one human bladder cancer cell line (TSU-Pr1, lane 4), and three human prostate cancer cell lines (DU145, PC-3, and LNCaP in lanes 2, 3 and 5, respectively), and six ovarian cancer cell lines (IOSE, BG-1, HEY, CAOv3, SKOV3 and NIH:OVCAR3 in lanes 6–11, respectively). The middle and bottom rows show the expression of β-tubulin and actin, respectively, as loading controls.

to the other. In doing so, we found that the percentage of epithelial cells stained by IHC in metastatic lesions was statistically as high as that in cancerous tissues.

Taken together, huMETCAM/MUC18 was highly expressed in both ovarian cancerous tissues and metastatic lesions, suggesting that it may be an indicator for the malignant potential of ovarian carcinomas. However, the positive correlation of the over-expression of METCAM/MUC18 with the advanced stages of ovarian cancer and metastatic lesions do not imply that METCAM/MUC18 is directly involved in the progression of ovarian cancers, which requires further testing the effect of METCAM/MUC18 on inducing tumorigenesis and metastasis.

Previously, the expression of huMETCAM/MUC18 in ovarian tissues had not been well studied because the mouse monoclonal antibodies used by other groups did not recognize the epitopes of the huMETCAM/MUC18 in ovarian tissues [15]. The positive results

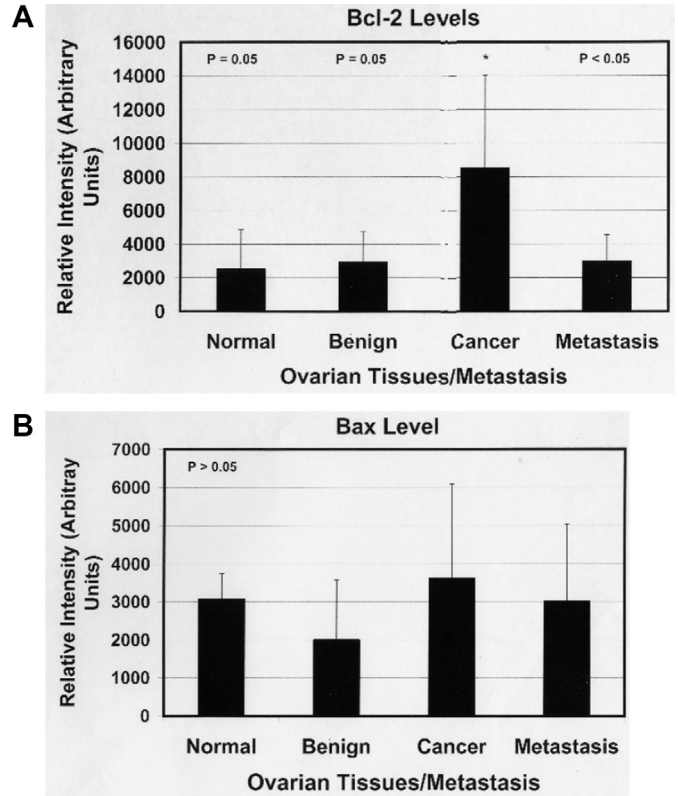


**Fig. 5.** Expression of (A) an antiapoptotic index (Bcl-2) and (B) a proapoptotic index (Bax) in ovarian tissues. The immunoblot analysis was carried out as described in the Materials and methods section: 30 µg protein of each tumor lysate was loaded per lane. The (A) Bcl2 (26 kDa) and (B) Bax (23 kDa) bands of the lysates of various ovarian tissues on the membranes were scanned, and the intensity of each band was determined. All the *p* values in (A) were calculated with respect to the reference data in the ovarian cancer tissues, as indicated by the asterisk. The *p* values in (B) was calculated with respect to the reference data in benign ovarian tissues.

**Table 2**

The level of huMETCAM/MUC18 expression in various ovarian cell lines and tissues versus that in one human melanoma cell line and three human prostate cancer cell lines.

Cell line/tissue	Cellular property	Origin of tissues	huMETCAM/MUC18 expression (%)	Tumor formation	Metastatic potential
IOSE	Preneoplastic ovarian epithelium	SV40-T antigen-immortalized ovarian epithelial cells	26 ± 2	None	None
CAOV-3	Ovarian cancer cell line	Human primary adenocarcinoma	50 ± 13	Yes	None?
HEY	Ovarian cancer cell line	Xenografted human moderately differentiated papillary cystadenocarcinoma	27 ± 3	Yes	None?
BG-1	Ovarian cancer cell line	Stage III human very poorly differentiated adenocarcinoma	0	Yes	None?
NIH:OVCAR3	Ovarian cancer cell line	Human malignant ascites	15 ± 3	Yes, ascites	Yes?
SK-OV-3	Ovarian cancer cell line	Human adenocarcinoma metastasis as malignant ascites	5 ± 2	Yes, ascites	Yes
CAOV-4	Ovarian cancer cell line	Human adenocarcinoma metastasis to subserosa fallopian tube	20	Yes	Yes
Human normal ovarian	Normal ovarian tissue	Human normal ovarian tissues	17.6 ± 9.5	None	None
Human benign ovarian adenoma	Benign ovarian	Human benign ovarian tissues	4.86 ± 3.99	None	None
Human ovarian cancer	Ovarian cancer (serous)	Human ovarian cancer	44.2 ± 28.4	Yes	Yes
Human metastasis lesion near ovaries	Metastatic lesions	Human ovarian metastasis	17.78 ± 14.8	Yes	Yes
SK-Mel-28	Melanoma cell line	Human malignant melanoma	100	Yes	Yes
DU145	Prostate cancer cell line	Brain metastasis	44 ± 5	Yes	Yes
PC-3	Prostate cancer cell line	Bone metastasis	25 ± 5	Yes	Yes
Tsu-PR1	Human bladder cancer		13 ± 2	Yes	Yes?
LNCaP	Prostate cancer cell line	Lymph node metastasis	0	Yes	None

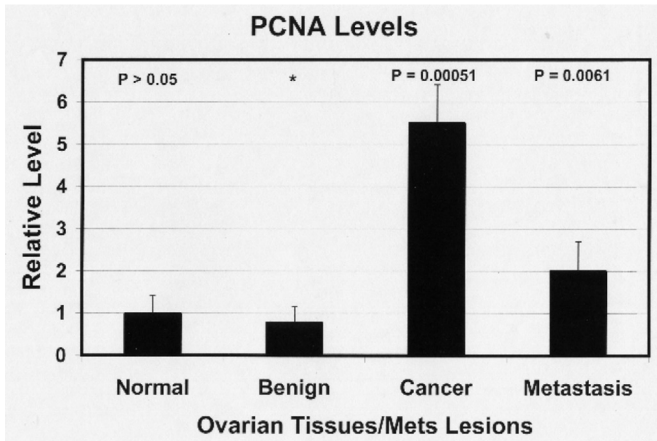


**Fig. 6.** Expression of a proliferate index (proliferating cell nuclear antigen, PCNA) in ovarian tissues. The PCNA (36 kDa) bands of the lysates of various ovarian tissues (30  $\mu$ g per lane) on the membranes were scanned and the intensity of each band were determined. All the *p* values were calculated with respect to the reference data in the benign ovarian tissues, as indicated by the asterisk.

in this report may be because of the polyclonal nature of our antibody, which recognizes multiple epitopes. In addition, the chicken antibody used here has a higher specificity than mouse monoclonal antibodies, as previously indicated [14,16,17,25–28].

To further investigate if the huMETCAM/MUC18 protein expressed in ovarian cancer tissues was similar to that in human ovarian cancer cell lines, we also used immunoblot analysis to determine the size of the protein in several ovarian cell lines. We showed that the apparent electrophoretic mobility of huMETCAM/MUC18 expressed in ovarian cancer cell lines was similar to that in ovarian tissues and that in a human melanoma cell line, SK-Mel-28, and in human melanoma, prostate, breast cancer, and bladder cancer cell lines. We suggest that post-translational modifications such as glycosylation in the protein expressed in ovarian tissues and ovarian cancer cell lines appear to be similar to that of other human cancer cell lines.

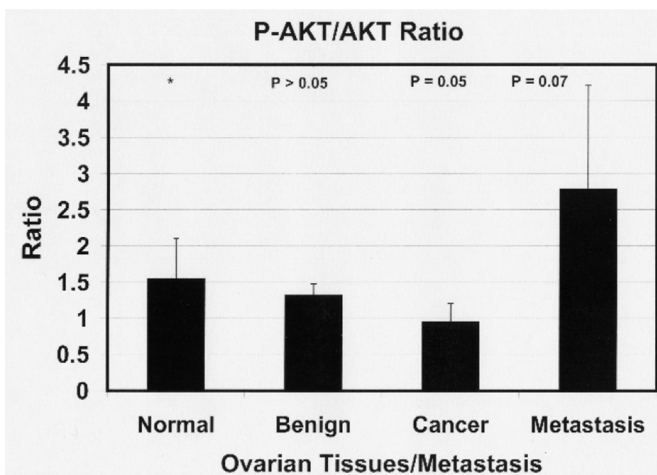


**Fig. 7.** Expression of a survival signal, ratio of phospho-AKT/AKT, in ovarian tissues. The AKT (60 kDa) and phospho-AKT (S473) (60 kDa) of the lysates of various ovarian tissues (30  $\mu$ g per lane) on the membranes were scanned, and the intensity of each band was determined. The ratio of phospho-AKT/AKT of each lysate was determined and is shown. All the *p* values were calculated with respect to the expression values of normal ovarian tissues, as indicated by the asterisk. The *p* values for each ovarian tissue are indicated.

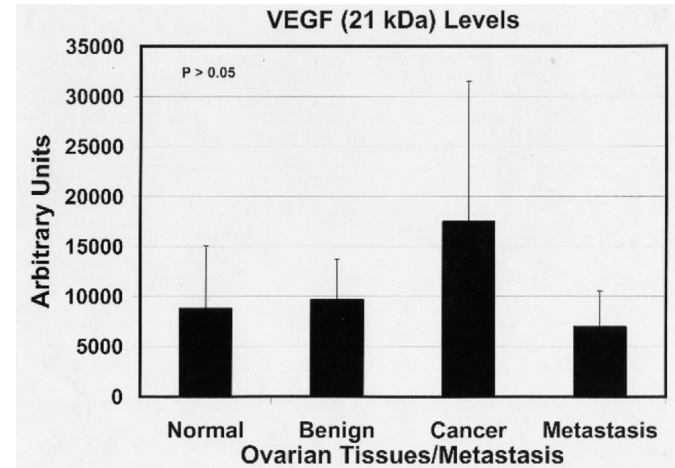


**Fig. 8.** Expression of vascular endothelial growth factor (VEGF) in ovarian tissues. The VEGF (21 kDa) bands of the lysates of various ovarian tissues (30  $\mu$ g per lane) on the membranes were scanned and the intensity of each band was determined.

HuMETCAM/MUC18 has been shown to increase the survival ability of prostate cancer cells by activating the AKT signaling pathway [36] and to increase tumor angiogenesis by increasing the expression of VEGF [37]. To be consistent with these notions, we found that an apoptotic index (Bax) was not statistically different in different ovarian tissues, but the levels of an anti-apoptotic index (Bcl2), a proliferate index (PCNA), and an angiogenesis index (VEGF) were all elevated in cancerous tissues compared to those in normal ovarian tissues and cystadenomas. The metastatic lesions had the highest levels of a key signaling index in the survival pathway, activated AKT, such as phospho-AKT (S473). From these results, we suggest that the elevated expression of huMETCAM/MUC18 protein may affect many downstream effectors, such as elevated anti-apoptotic activity, proliferative ability, angiogenesis, and the activation of signaling in cell survival pathways, which contributes significantly to the progression of clinical ovarian cancer [34–39]. The results are also consistent with the published results that expression of PCNA [39], activation of AKT signaling [36], and expression of VEGF [37] are increased in ovarian cancers. Taken together, the overexpression of huMETCAM/MUC18 in ovarian cancer tissues may indicate its role in promoting tumorigenesis and in initiating the metastasis of human ovarian cancer cells via these mechanisms.

## Conclusion

METCAM/MUC18 was overexpressed in ovarian carcinomas and ovarian metastatic lesions, but not in normal ovarian tissues and cystadenomas. This correlation of higher levels of huMETCAM/MUC18 expression in the ovarian cancers may be used as a diagnostic marker to differentiate ovarian cancer from benign cystadenomas. Our findings may also be used for the prediction of the malignant potential of epithelial ovarian cancer; however, this does not mean that METCAM/MUC18 plays a direct role in the malignant progression of human ovarian cancer cells and we do not suggest that METCAM/MUC18 plays a role in the malignant progression of cystadenomas to ovarian cancers. In summary, our findings are consistent with the observations in a recent report [40], which suggested that METCAM/MUC18 may be a marker of poor prognosis in epithelial ovarian cancer [40]; in addition we also studied possible pathways involved in the malignant progression of this cancer.



## Conflicts of interest

The authors have no conflicts of interest relevant to this article.

## Acknowledgments

This work was supported in part by the intramural bridge funding from Emory University School of Medicine and in part by a grant from the Emory University Research committee (GJW) and in part by a grant from National Science Council (NSC-101-2320-B-033-001&003), Taiwan. This work was also partly supported by funds from the Ovarian Cancer Coalition (EBD). We thank Mr Eugene Lee Son and Mrs Mei-Whey H. Wu for their excellent technical help. We thank Dr John F. McDonald for access to the tissues from the Northside Hospital given to the Ovarian Cancer Institute at the Georgia Institute of Technology. We thank Drs Cynthia Cohen and Sanjay Logani for the access to the Ovarian Tissue Bank at Emory University Hospital. We thank Dr Nelly Auersperg for the IOSE cell line. We thank Dr N.J. Bowen for his assistance with the ONCOMINE analysis. We also thank Mr Jonathan Wu for editing the English in this manuscript.

## References

- [1] Jemal A, Siegel R, Ward E, Murray T, Xu J, Smigal C, Thun MJ. Cancer Statistics, 2006. *CA Cancer J Clin* 2006;56:106–30.
- [2] Adib TR, Henderson S, Perrett C, Hewitt D, Bourmpoulia D, Ledermann J, et al. Predicting biomarkers for ovarian cancer using gene-expression microarrays. *Br J Cancer* 2004;90:686–92.
- [3] McCluggage WG, Wilkinson N. Metastatic neoplasms involving the ovary: A review with an emphasis on morphological and immunohistochemical features. *Histopathology* 2005;47:231–47.
- [4] Cavallaro U, Christofori G. Cell adhesion and signaling by cadherins and Ig-CAMs in cancer. *Nature Rev Cancer* 2004;4:118–32.
- [5] Sundfeldt K. Cell-cell adhesion in the normal ovary and ovarian tumors of epithelial origin; an exception to the rule. *Mol Cell Endocrinol* 2003;202:89–96.
- [6] Burleson KM, Casey RC, Skubitz KM, Pambuccian SE, Oegema Jr TR, Skubitz APN. Ovarian carcinoma ascites spheroids adhere to extracellular matrix components and mesothelial cell monolayers. *Gynecol Oncol* 2004;93:170–81.
- [7] Rump A, Morikawa Y, Tanaka M, Minami S, Umesaki N, Takeuchi M, et al. Binding of ovarian cancer antigen CA125/MUC16 to mesothelium mediates cell adhesion. *J Biol Chem* 2004;279:9190–8.
- [8] Strobel T, Cannistra SA.  $\alpha$ 1-Integrins partly mediate binding of ovarian cancer cells to peritoneal mesothelium in vitro. *Gynecol Oncol* 2004;73:362–7.
- [9] Bourguignon LYW, Gilad E, Rothman K, Peyrollier K. Hyaluronan-CD44 interaction with IQGAP1 promotes Cdc42 and ERK signaling, leading to actin binding, Elk-1/estrogen receptor transcription activation, and ovarian cancer progression. *J Biol Chem* 2005;280:11961–72.
- [10] Euer NI, Kaul S, Deissler H, Mobus VJ, Zeillinger R, Weidle UH. Identification of L1CAM, Jagged2, and neuromedin U as ovarian cancer-associated antigens. *Oncol Reports* 2005;13:375–87.
- [11] Imai T, Horiuchi A, Shiozawa T, Osada R, Kikuchi N, Ohira S. Elevated expression of E-cadherin and alpha-, beta-, and gamma-catenins in metastatic lesions compared with primary epithelial ovarian carcinomas. *Human Pathol* 2004;35:1469–76.
- [12] D'Souza T, Agarwal R, Morin PJ. Phosphorylation of claudin-3 at threonine 192 by cAMP-dependent protein kinase regulates tight junction barrier function in ovarian cancer cells. *J Biol Chem* 2005;280:26233–40.
- [13] Lehmann JM, Reithmuller G, Johnson JP. MUC18, a marker of tumor progression in human melanoma. *Proc Natl Acad Sci USA* 1989;86:9891–5.
- [14] Wu GJ. METCAM/MUC18 expression and cancer metastasis. *Curr Genomics* 2005;6:333–49.
- [15] Shih IM. The role of CD146 (Mel-CAM) in biology and pathology. *J Pathol* 1999;189:4–11.
- [16] Wu GJ, Varma VA, Wu MWH, Yang H, Wang SWC, Liu Z, et al. Expression of a human cell adhesion molecule, MUC18, in prostate cancer cell lines and tissues. *Prostate* 2001;48:305–15.
- [17] Wu GJ, Wu MWH, Wang SW, Liu Z, Peng Q, Qu P, et al. Isolation and characterization of the major form of human MUC18 cDNA gene and correlation of MUC18 over-expression in prostate cancer cells and tissues with malignant progression. *Gene* 2001;279:17–31.
- [18] Wu GJ, Fu P, Chiang CF, Hess W, Greenberg NM, Wu MWH. Increased expression of MUC18 correlates with the metastatic progression of mouse prostate adenocarcinoma in the TRAMP model. *J Urol* 2005;173:1778–83.
- [19] Chiang CF, Son EL, Wu GJ. Oral treatment of male TRAMP mice with doxazosin suppresses prostate tumor growth and metastasis. *Prostate* 2005;64:408–18.
- [20] Xie S, Luca M, Huang S, Gutman M, Reich R, Johnson JP, et al. Expression of MCAM/MUC18 by human melanoma cells leads to increased tumor growth and metastasis. *Cancer Res* 1997;57:2295–303.
- [21] Schlagbauer-Wadl H, Jansen B, Muller M, Polterauer P, Wolff K, Eichler HG, et al. Influence of MUC18/MCAM/CD146 expression on human melanoma growth and metastasis in SCID mice. *Int J Cancer* 1999;81:951–5.
- [22] Wu GJ, Fu P, Wang SW, Wu MWH. Enforced expression of MCAM/MUC18 increases in vitro motility and invasiveness and in vivo metastasis of two mouse melanoma K1735 sublines in a syngeneic mouse model. *Mol Cancer Res* 2008;6:1666–77.
- [23] Yang H, Wang SWC, Liu Z, Wu MWH, McAlpine B, Ansel J, et al. Isolation and characterization of murine MUC18 cDNA gene, and correlation of MUC18 expression in murine melanoma cell lines with metastatic ability. *Gene* 2001;265:133–45.
- [24] Wu GJ, Peng Q, Fu P, Wang SWC, Chiang FCF, Dillehay DL, et al. Ectopical expression of human MUC18 increases metastasis of human prostate cancer cells. *Gene* 2004;327:201–13.
- [25] Wu GJ. The role of MUC18 in prostate carcinoma. In: Hayat MA, editor. *Immunohistochemistry and in situ hybridization of human carcinoma. Molecular pathology, lung carcinoma, breast carcinoma, and prostate carcinoma, vol. 2.* Elsevier Science/Academic Press; 2004. p. 347–58.
- [26] Wu GJ, Wu MWH, Liu Y. Enforced expression of human METCAM/MUC18 increases the tumorigenesis of human prostate cancer cells in nude mice. *J Urol* 2011;185:1504–12.
- [27] Zeng GF, Cai SX, Wu GJ. Up-regulation of METCAM/MUC18 promotes motility, invasion, and tumorigenesis of human breast cancer cells. *BMC Cancer* 2011;11:113. <http://dx.doi.org/10.1186/1471-2407-11-113>. 30 March 2011.
- [28] Zeng GF, Cai SX, Liu Y, Wu GJ. METCAM/MUC18 augments migration, invasion, and tumorigenicity of human breast cancer SK-BR-3 cells. *Gene* 2012;492:229–38.
- [29] Zeng Q, Li W, Lu D, Wu Z, Duan H, Luo Y, et al. CD146, an epithelial-mesenchymal transition inducer, is associated with triple-negative breast cancer. *Proc Natl Acad Sci USA* 2012;109:1127–32.
- [30] McGary EC, Heimberger A, Mills L, Weber K, Thomas GW, Shtivelband M, et al. A fully human anti-melanoma cellular adhesion molecule/MUC18 antibody inhibits spontaneous pulmonary metastasis of osteosarcoma cells in vivo. *Clin Cancer Res* 2003;9:6560–6.
- [31] Vogelstein B, Kinzler KW. Cancer genes and the pathways they control. *Nature Med* 2004;10:789–99.
- [32] Auersperg N, Maines-Bandiera SL, Dyck HG, Kruk PA. Characterization of cultured human ovarian surface epithelial cells (IOSE): phenotypic plasticity and premalignant changes. *Lab Invest* 1994;71:510–8.
- [33] Geisinger KR, Kute TE, Pettenati MJ, Welander CE, Dennard Y, Collins LA, et al. Characterization of a human ovarian carcinoma cell line, BG-1, with estrogen and progesterone receptors. *Cancer* 1989;63:280–8.
- [34] Buick RN, Pullano R, Trent JM. Comparative properties of five human ovarian adenocarcinoma cell lines. *Cancer Res* 1985;45:3668–76.
- [35] Hanahan D, Weinberg RA. The hallmarks of cancer: the next generation. *Cell* 2011;144:646–74.
- [36] Yuan ZQ, Sun M, Feldman RI, Wang G, Ma X, Jiang C, et al. Frequent activation of AKT2 and induction of apoptosis by inhibition of phosphoinositide-3-OH kinase/Akt pathway in human ovarian cancer. *Oncogene* 2000;19:2324–30.
- [37] Rasila KK, Burger RA, Smith H, Lee FC, Verschraegen C. Angiogenesis in gynecological oncology—mechanism of tumor progression and therapeutic targets. *Int J Gynecol Cancer* 2005;15:710–26.
- [38] Naora H, Montell DJ. Ovarian cancer metastasis: integrating insights from disparate model organisms. *Nature Reviews/Cancer* 2005;5:355–66.
- [39] Warrenfeltz S, Pavlik S, Datta S, Kraemer ET, Benigno B, McDonald JF. Gene expression profiling of epithelial ovarian tumors correlated with malignant potential. *Mol Cancer* 2004;3:27–43.
- [40] Aldovini D, Demichelis F, Doglioni C, Di Vizio D, Galligioni E, Brugnara S, et al. M-cam expression as marker of poor prognosis in epithelial ovarian cancer. *Int J Cancer* 2006;119:1920–6.